

AperTO - Archivio Istituzionale Open Access dell'Università di Torino

A comparative study of myocardial molecular phenotypes of two tfr2 β null mice: Role in ischemia/reperfusion

This is a pre print version of the following article:

Original Citation:

Availability:

This version is available <http://hdl.handle.net/2318/1539490> since 2016-06-23T01:55:39Z

Published version:

DOI:10.1002/biof.1237

Terms of use:

Open Access

Anyone can freely access the full text of works made available as "Open Access". Works made available under a Creative Commons license can be used according to the terms and conditions of said license. Use of all other works requires consent of the right holder (author or publisher) if not exempted from copyright protection by the applicable law.

(Article begins on next page)



UNIVERSITÀ DEGLI STUDI DI TORINO

This is an author version of the contribution published on:

Questa è la versione dell'autore dell'opera:

[Biofactors. 2015 Sep-Oct;41(5):360-71. doi: 10.1002/biof.1237. Epub 2015 Oct 13.

]

.

The definitive version is available at:

La versione definitiva è disponibile alla URL:

<http://onlinelibrary.wiley.com/doi/10.1002/biof.1237/full>

A Comparative Study of Myocardial Molecular Phenotypes of Two Tfr2 β Null Mice: Role in Ischemia/Reperfusion

**Martina Boero[#], Pasquale Pagliaro^{*#}, Francesca Tullio, Rosa M. Pellegrino, Antonietta Palmieri,
Ludovica Ferbo, Giuseppe Saglio, Marco De Gobbi, Claudia Penna[#], Antonella Roetto^{*#}**

¹University of Torino, Department of Clinical and Biological Sciences, AOU San Luigi Gonzaga, Orbassano, Torino, Italy, ²National Institute for Cardiovascular Researches (INRC), Bologna, Italy.

These authors contributed equally to this work

Running Head: **Myocardial Molecular Phenotype of Tfr2 β Null Mice**

* Corresponding Authors

Pasquale Pagliaro, Antonella Roetto
Department of Clinical and Biological Sciences,
AOU San Luigi Gonzaga, Regione Gonzole, 10,
10043 Orbassano, Italy University of Torino
pasquale.pagliaro@unito.it, antonella.roetto@unito.it

Abstract

Transferrin receptor 2 (Tfr2) is an iron-modulator transcribed in two isoforms, Tfr2 α and Tfr2 β . The latter is expressed in the heart. We obtained two mouse models with silencing of Tfr2 β : one with a normal systemic iron amount (SIA), *i.e.* Tfr2-KI, and the other, *i.e.* LCKO-KI, with high SIA due to hepatic Tfr2 α silencing. We aimed to assess whether Tfr2 β might play a role in myocardial injury and whether Tfr2 β silencing might modify proteins of iron metabolism, antioxidant, apoptotic and survival enzyme activities in the heart undergoing ischemia/reperfusion (I/R).

Isolated hearts of wild-type (WT) and Tfr2-null mice were studied before or after an I/R protocol, and proteins/RNA analyzed by Western blot and/or quantitative PCR.

Tfr2 β increased in WT hearts subject to I/R, and both Tfr2 β null mice hearts were protected against I/R injury (about 40% smaller infarct-size compared to WT hearts). RISK kinases (ERK1/2-AKT-PKC ϵ) were found up-regulated after I/R in Tfr2-KI, whereas SAFE enzyme (Stat3) and GSK3 β resulted phosphorylated during I/R in LCKO-KI hearts. While HO-1 and HIF-2 α were high in both Tfr2 β -null mice, Catalase and pro-apoptotic factors were upregulated only in LCKO-KI. Finally, Tfr2-KI hearts presented an increased Ferritin-H and a decreased Ferroportin1, whereas LCKO-KI hearts displayed an upregulation of Ferritin-L chain and DMT1/Hamp-RNA.

In conclusion, Tfr2 β isoform is involved in cardiac iron metabolism and its silencing leads to a protected phenotype (antioxidants, RISK and/or SAFE upregulation) against I/R challenging. Iron-dependent signals involved in cardioprotection seem to be positively affected by Tfr2 β downregulation and subsequent Ferritins upregulation.

Key words: Ferritin, Iron; RISK; SAFE; Transferrin receptor; Transgenic model.

List of abbreviations:

DMT1, Divalent Metal Transporter 1

ERK 1/2, Extracellular-Signal-Regulated Kinases 1/2

FtH , Ferritin H

FtL, Ferritin L

Fpn1, Ferroportin 1

GSK3 β , Glycogen Synthase Kinase 3 β

HIC, Heart Iron Concentration

HO-1, Heme Oxygenase-1

Hamp, Hepcidin

HIF-2a, Hypoxia-Inducible Factor-2a

IS, Infarct Size

IRE/IRP, Iron Responsive Elements /Iron Regulatory Proteins

I/R, Ischemia/Reperfusion

PKB or AKT, Protein Kinase B

PKC ϵ , Protein Kinase C ϵ

ROS, Reactive Oxygen Species

RISK, Reperfusion Injury Salvage Kinases

Stat3, Signal Transducer and Activator of Transcription 3

SOD1, Superoxide Dismutase

SAFE, Survivor Activating Factor Enhancement

SIA, Systemic Iron Amount

Tfr2, Transferrin Receptor 2

WT, Wild-type

1. Introduction

Iron is essential for the optimal functioning and survival of living beings. It is indispensable for the maintenance of cellular energy and metabolism of all tissues [1]. However, when iron accumulates in cells, it contributes to reactive oxygen species (ROS) formation through the Fenton/Haber-Weiss reactions generating *oxidative stress* [2,3]. Heart, together with liver, duodenum and bone marrow, is an organ in which iron metabolism must be tightly regulated. In fact, individuals with iron overload associated diseases, like hemoglobinopathy and hemochromatosis, can present signs of heart failure [4].

TFR2 (Transferrin Receptor 2) is a gene involved in iron metabolism transcribed in two main isoforms: the hepatic- and erythroid-specific full length Tfr2 α and the ubiquitous shorter form Tfr2 β [5]. In the liver it is a regulator of hepatic hepcidin (Hamp) protein, the hormone that control iron systemic availability inhibiting the functionality of the cellular iron exporter Ferroportin 1 (Fpn1) [6]. On the contrary, the Tfr2 β isoform is expressed in all tissues [5] and its function is not well understood yet. It seems to be involved in Fpn1 transcription up-regulation, although it is not involved in direct iron export from cells [7].

Since Tfr2 β resulted to be highly transcribed in heart [5], as well as Hepcidin (Hamp) [8] and Ferroportin 1 (Fpn1) [9] genes, we planned to investigate if Tfr2 β isoform could have some role in cardiac iron homeostasis and in myocardial injury during stress. To this aim, two animal models, Tfr2-KI and Tfr2 LCKO-KI, with germinal and conditional silencing of the Tfr2 gene isoforms [7] were produced. The two Tfr2-targeted mice have a germinal silencing of Tfr2 β isoform, whereas Tfr2 LCKO-KI animals have also an hepatic selective silencing of the Tfr2 α .

Therefore in hearts these two Tfr2 β null mice models are both Tfr2 β null, but they have a different systemic iron amount. In fact the first, Tfr2-KI, has normal serum iron parameters while the latter, Tfr2 LCKO-KI has high serum ferritin and transferrin saturation [7]. Accordingly, Tfr2 LCKO-KI is a severe hepatic iron overloaded mouse model, whereas Tfr2-KI has normal tissue iron amount in liver

but increased iron deposit in spleen [7]. These differences may help to clarify the relative importance of systemic iron overload in cardiac response to stress. Although it is unknown the impact of these Tfr2 gene modifications on the heart iron concentration (HIC), we hypothesized a different cardiac cell survival and resistance to stressful stimuli in these two models. In particular, we hypothesized that the iron overloaded model is more prone to cardiac damage due to iron-dependent redox stress.

To test these hypotheses and to explore the relevance of Tfr2 β in cardiac iron content and metabolism we used Ischemia/Reperfusion (I/R) protocol as a stress stimulus in hearts of Tfr2-KI and Tfr2 LCKO-KI mice as well as in WT mice hearts.

Several studies, in the setting of I/R evolving to myocardial infarction, have demonstrated that cardioprotection involves cell metabolism modifications and that it is mainly mediated by the activation of two independent or cross-talking cardioprotective *redox sensible* pathways in which iron may play a role: Reperfusion Injury Salvage Kinases (RISK) that includes AKT/PKB and ERK1/2, and Survivor Activating Factor Enhancement (SAFE) that involves Signal Transducer and Activator of Transcription 3 (Stat3) [10-16]. Moreover, the up-regulation of RISK and/or SAFE kinases has also been observed in transgenic mice for different proteins, which resulted endogenously preconditioned and protected from I/R damage [12, 17].

Furthermore, since endogenous enzymes regulate the homeostasis of ROS with an iron dependent mechanism, we studied in our models of I/R the expression of superoxide dismutase (SOD1) and Catalase, which are well known anti-oxidant enzymes involved in the conversion of superoxide radical ($O_2^{\cdot -}$) to hydrogen peroxide (H_2O_2) and in the maintenance of steady-state levels of H_2O_2 , respectively [18,19]. Moreover, in order to deepen cardiac iron dependent redox setting, before and after I/R procedure, we analyzed HO1 and HIF-2 α , whose levels have been demonstrated to be influenced by iron dependent redox conditions [20, 21]. Finally, since apoptosis is tightly correlated to redox stress, *anti- and pro-apoptotic enzymes* have been considered.

Therefore the aims of the present study were: 1) to evaluate if Tfr2 β production is influenced by I/R in WT mice, 2) to assessed if the lack of Tfr2 β expression (with and without systemic iron overload)

induces some variation on I/R injury in isolated hearts, 3) to investigate whether Tfr2 β silencing modifies antioxidant, apoptotic and survival (RISK/SAFE) enzymes activity; 4) to analyze pre- and post-ischemic levels of HIC and main iron proteins (Hamp, Fpn1, DMT1, HIF-2a and Ferritins) in hearts of each Tfr2 targeted mice compared to WT controls.

2. Experimental Procedures

2.1. Animals

Male 10 week old wild-type (WT, sv 129) and transgenic Tfr2 β null, KI and LCKO-KI (Tfr2 liver KO mice in a KI background) mice received humane care in compliance with Italian law (DL-26, Mar 04, 2014) and in accordance with the EU Directive 2010/63/EU and approved by the University of Turin Ethical Committee for animal research and by the Italian Ministry of Health. All efforts were made to minimize suffering. Animals plasmatic transferrin saturation was calculated as a ratio of serum iron and total iron binding capacity levels (Randox Laboratories Ltd., UK).

Tfr2 transgenic mice (KI and LCKO-KI) and WT sib-pairs weighing between 20-30 g were given 500 U heparin and anesthetized (Tribromoethanol; Sigma-Aldrich) (50 mg/kg) by intra-peritoneal injections before being culled by cervical dislocation [22].

2.2. Isolated Heart

Hearts were rapidly excised and retrogradely perfused at 80 mmHg by the Langendorff technique with Krebs–Henseleit bicarbonate buffer containing (mM) NaCl 118, NaHCO₃ 25, KCl 4.7, KH₂PO₄ 1.2, MgSO₄ 1.2, CaCl₂ 1.25, and Glucose 11. The buffer was gassed with 95% O₂, 5% CO₂. The temperature of the perfusion system was maintained at 37°C. The perfusate flowing out of the heart was collected and measured [12,23]. At the end of experimental protocol, hearts were used for molecular analyses and infarct size assessment (see below).

2.2.1. Experimental protocol

To have a reference group (WT I/R, n= 6), hearts were harvested from the WT animals, perfused and allowed to stabilize for 30-min. After stabilization period, hearts were subjected to a protocol of I/R,

which consisted in 30-min of global no-flow, normothermic ischemia and a period of 60-min of reperfusion [12].

Similarly transgenic hearts (KI I/R, n=7; and LCKO-KI I/R, n=5) were perfused for a 30-min stabilization period, then global normothermic ischemia was applied by eliminating flow for 30-min, which was followed by 60-min reperfusion [12].

2.2.2. Infarct size assessment

Infarct areas were assessed at the end of the experiments with the nitro-blu-tetrazolium technique in a blinded fashion, as previously described [12]. In brief, immediately after reperfusion hearts were removed from the perfusion apparatus and the left ventricle (LV) dissected by transverse sections into three slices (<1 mm slices). Following 20 min of incubation at 37°C in 0.1% solution of nitro-blu-tetrazolium (Sigma-Aldrich) in phosphate buffer, unstained necrotic tissue was carefully separated from stained viable tissue by an independent observer, who was unaware of the protocols. The necrotic mass was expressed as a percentage of risk area (*i.e.* total left ventricular mass) [12].

2.3. Molecular biology analysis

Five additional hearts of each group (WT I/R, KI I/R and LCKO-KI I/R) underwent I/R protocols and used for molecular studies. Moreover, five hearts of each group (WT Sham, KI Sham and LCKO-KI Sham) after 30-min stabilization underwent 90-min buffer-perfusion only and served as reference non-ischemic groups for molecular studies. Frozen LV of I/R and Sham groups were used for Western blot and/or quantitative PCR analysis of iron protein tool kit (*i.e.* Ferritins, Hamp, Fpn1, DMT1, HO-1 and HIF-2a), antioxidants (Catalase and SOD1), apoptotic or RISK (AKT, ERK1/2; PKC ϵ and GSK3 β) and SAFE (Stat3 and GSK3 β) elements (see also below).

2.3.1. Real time quantitative PCR analysis

For reverse transcription, 1 μ g of total RNA, 25 μ M random hexamers, and 100 U of reverse transcriptase (Applera) were used. Gene expression levels were measured by real-time quantitative PCR in an iCycler (Bio-Rad) using commercial assays (Assays-on Demand; Applied Biosystems) for Hamp and Fpn1 gene transcription evaluation. β -actin gene was utilized as housekeeping control. The

results were analyzed using the $\Delta\Delta^{Ct}$ method [24]. All analyses were carried out in triplicate; results showing a discrepancy greater than one cycle threshold in one of the wells were excluded.

2.3.2. Western blot analysis

For Western blotting, hearts were lysed in Tris-buffered saline with 1% Triton X-100 plus (1% SDS added for Tfr2 β protein WB), complete protease inhibitor cocktail (Roche). Protein extracts were clarified with three sequential centrifugations for 20 minutes at 20,000 g, at 4°C. Between 50 and 100 μ g of proteins from homogenized heart tissue were electrophoresed in 8% to 10% SDS polyacrylamide gel electrophoresis and immunoblotted according to standard protocols. Antibodies against the following proteins were used: AKT, p-AKT(Ser473), GSK3 β , pGSK3 β (Ser9), PKC ϵ , pStat3 (Tyr705) (*Cell Signaling*); ERK1/2, pERK1/2 (Thr202), Stat3 (F-2), Tfr2 S-20, Transferrin Receptor 1 (Tfr,CD71 (H300), Gapdh (A3), DMT1 (H-108) HO-1 (H-105) and BCL-XL (H-S) (*Santa Cruz Biotechnology*); pPKC ϵ (Ser729) SOD1 and Catalase (*Thermo Scientific*). HIF-2a antibody (HIF-2A11-A) was from Alpha Diagnostic. Antibodies against the two isoforms of Ferritin (FtH and FtL) were kindly provided by Sonia Levi, University of Vita Salute, Milan Italy. Protein quantification was done using Protein Assay (Biorad). In brief, WB were developed utilizing clarity western ECL substrate (Biorad) and the chemidoc XRS+Instrument (Biorad). Proteins amount, evidenced by band intensity, was measured by densitometry with a band quantification software (Image lab software, Biorad). Each protein amount was normalized for its own Gapdh amount and final protein quantification were obtained as the mean of all the samples analyzed for each of the 6 experimental group, and expressed as fold increase, relative to the mean obtained from the WT mice.

Gapdh is considered an appropriate loading control as it has been shown to change under iron deficiency, but not under iron normal/overload conditions [25], which are typical conditions of our experimental models.

2.4. Cardiac iron content

Heart Iron Concentration (HIC) was assessed according to standard procedure [7] using 20 mg of dried LV. A minimum of 5 samples have been analyzed for each Sham and I/R group.

2.5. Statistical analysis

Statistical significance of the differences between Sham WT and each Sham targeted mice was evaluated using a Student *t* test (unpaired, 2 tailed). Also significance of the differences between the two I/R groups or between I/R and correspondent Sham group was evaluated using a Student *t* test (unpaired, 2 tailed). Results are shown as medium values \pm standard error. $p < 0.05$ was considered significant.

3. Results

We confirmed that Tfr2 targeted mice used in these experiments present the same phenotype of the original report [7]. In particular, transferrin saturation resulted normal (30 ± 5 %) in Tfr2-KI and very high (80 ± 12 %) in Tfr2 LCKO-KI, thus confirming the condition of iron overload in the latter model.

3.1. Role of Tfr2 β in myocardial injury (Fig 1)

To ascertain whether or not Tfr2 β may play a role in myocardial injury, we studied how Tfr2 β expression changes immediately after I/R experiment in WT. As shown in figure 1a, I/R procedure significantly increased Tfr2 β protein level compared to Sham.

To evaluate the effect of the absence of Tfr2 β on myocardial I/R injury, we measured infarct size in WT, Tfr2-KI and LCKO-KI hearts (Fig 1b). Total infarct size is expressed as a percentage of LV mass. As shown in figure 1b, infarct size was significantly lower in Tfr2-KI (infarct size $37 \pm 6\%$, $p < 0.05$) and LCKO-KI ($36 \pm 6\%$, $p < 0.05$) compared to WT hearts ($58 \pm 3\%$). Moreover, apoptosis has been evaluated through analysis of apoptotic markers BCL-X as a ratio of BCL-XS (pro-apoptotic) and BCL-XL (anti-apoptotic) isoforms [26], in Sham and I/R conditions. BCL-X S/L ratio resulted to be decreased in Tfr2-KI and increased in Tfr2 LCKO-KI Sham hearts compared to WT (Figure 1c). Yet, levels of pro-apoptotic factor were not modified by acute I/R protocols.

Therefore, both Tfr2 β null mice hearts were protected against I/R injury (about 40% smaller infarct-size in transgenic models compared to WT hearts; Fig 1b), regardless the difference in terms of apoptosis in baseline conditions.

3.2. Identification of cellular pathways of protection in Tfr2 β null hearts

3.2.1. Cardioprotective enzyme HO-1 is increased in Tfr2 β null mice hearts (Fig 1d)

Heme oxygenase-1 (HO-1) is an enzyme involved in heme catabolism that increases in response to oxidative stress [27]. It has been demonstrated to have a role as a marker of cytoprotection [28] and in particular to be cardioprotective against I/R injury [29]. HO-1 resulted to be significantly higher in both Tfr2 β null mice Sham hearts compared to WT hearts. Moreover HO-1 levels were significantly lower in KI I/R hearts with respect to KI Sham only.

3.2.2. HIF2a is upregulated in hearts of transgenic models and changes differently in WT and Tfr2 targeted animals after I/R (Fig 1e)

Since Hypoxia-Inducible Factor-2a (HIF2a) levels are influenced by iron, ROS and hypoxia, we analyzed the levels of HIF2a with and without I/R in our models. HIF2a protein resulted upregulated in both Tfr2 β null Sham hearts ($p < 0.05$ vs WT Sham). However, after I/R procedure, while HIF2a tended to increase in WT, it decreased in Tfr2-KI ($p < 0.01$ vs KI Sham) and tended to decrease in LCKO-KI (Fig 1f).

3.3. RISK and SAFE in non-ischemic and ischemic hearts

To assess possible mechanisms involved in cardioprotection exerted by the lack of Tfr2 β in Tfr2-KI and LCKO-KI, enzymes of major pro-survival signaling pathways were investigated by Western blot analysis in samples collected from hearts subject to I/R stress or Sham perfusion.

3.3.1. RISK and/or SAFE are minimally altered in Sham hearts of transgenic models (Figs 2 and 3)

In the three Sham groups, ERK1/2, AKT and PKC, as well as Stat3 and GSK3 β (RISK- and SAFE-pathways) displayed similar phosphorylation ratios (Figures 2 and 3). However some peculiarities

were found: while ERK 1/2 (Fig 3a) resulted significantly lower ($p < 0.01$) in the Sham groups of Tfr2-KI compared to WT, Stat3 resulted significantly lower ($p < 0.05$) in LCKO-KI Sham group (Figure 3a).

3.3.2. *RISK and/or SAFE are activated by I/R in transgenic models (Figs 2 and 3)*

We then analyzed the effect of I/R in the RISK- and SAFE-pathways. As shown in Fig 3, whereas in WT the I/R protocol induced a reduction of ERK1/2 phosphorylation ($p < 0.001$ vs WT Sham, panel a), in Tfr2-KI an increase of ERK1/2, AKT and PKC ϵ phosphorylation (panels a, b, and c), was seen after I/R compared to the Sham group ($p < 0.05$ vs KI Sham). Moreover, in LCKO-KI, phosphorylation of Stat3 (Figure 3a), a crucial factor of the SAFE pathway, and phosphorylation of the down-stream kinase GSK3 β (Figure 3b) were induced by I/R ($p < 0.01$ vs LCKO-KI Sham groups).

3.4. Antioxidants, iron content and iron proteins in non-ischemic and ischemic hearts

3.4.1. *Antioxidant enzymes are differently regulated in Tfr2 β null mice (Fig 4)*

Intriguingly, the level of the antioxidant Catalase resulted significantly higher ($p < 0.05$) in Tfr2 LCKO-KI Sham and I/R as compared to WT (Sham and I/R) and KI hearts (Figure 4). On the contrary, the levels of SOD1 were not significantly modified (data not shown).

3.4.2. *Cardiac iron proteins change as a consequence of Tfr2 targeting and after I/R procedure in WT and transgenic models (Fig 5).*

Transcription analysis of Cardiac Hamp and Fpn1 revealed that Tfr2-KI and LCKO-KI presented different Hamp and Fpn1 levels in untreated mice hearts (Sham) compared to WT Sham and different responses to the I/R procedure. In particular, Hamp transcription was higher in LCKO-KI Sham hearts compared to WT hearts ($p < 0.05$; Fig 5a). On the contrary, cardiac Fpn1 transcription was lower in both Tfr2-KI and LCKO-KI Sham hearts compared to WT Sham hearts ($p < 0.05$ vs KI only; Fig 5b).

I/R procedure did not influence significantly Hamp and Fpn1 transcription; however, Hamp transcription tended to increase in the three groups (Fig 5a), whereas Fpn1 transcription tended to decrease in WT and Tfr2 LCKO-KI hearts only (Fig 5b).

No significant variation could be seen in cardiac Fpn1 protein amount in Sham and I/R (not shown) while iron importer Divalent Metal Transporter 1 (DMT1) resulted to be significantly increased only in Tfr2 LCKO-KI Sham and I/R hearts (Fig 5c).

3.4.3. Heart iron concentration tends to vary differently in WT and Tfr2 targeted animals after I/R (Fig 6a)

Heart Iron Concentration (HIC) evaluation did not reach significant differences among different groups. However, after I/R procedure there was a tendency to a lower HIC in WT and LCKO-KI hearts compared to their Sham group. (Fig 6a).

3.4.4. Ferritin H and L change differently in the two Tfr2 targeted animals (Fig 6b and 6c)

Ferritin H (FtH) amount revealed a significant increase in Tfr2-KI Sham hearts vs WT Sham ($p < 0.05$, Fig 6b). On the contrary Ferritin L (FtL) tended to be higher in LCKO-KI Sham hearts vs WT Sham ($p = 0.09$, Fig 6c). Although FtL in LCKO-KI I/R resulted higher than WT I/R, the I/R procedure did not influence significantly the amounts of the two Ferritins when compared to Sham groups, in the three models.

4. Discussion

We aimed to study the putative role of Tfr2 β isoform in hearts using Tfr2 β null animal models and determining molecular phenotype of the myocardium before and after a stress challenging, namely I/R. This study strongly indicates that while hearts of WT mice exposed to I/R increase the expression of Tfr2 β , hearts of Tfr2 β null mice modify the molecular phenotype and display an increased tolerance to I/R challenging.

Transferrin receptor 2 is a gene that codifies for two proteins (Tfr2 α and Tfr2 β) involved in iron metabolism whose mutations are observed in type 3 hemochromatosis (HFE3), an iron overload genetic disorder [30]. Tfr2 β in particular, is a protein well expressed in cardiac tissue [5] whose function is related to modulation of iron export from cells regulating the transcription of iron exporter

Fpn1 [7], while Tfr2 alpha is an iron sensor that contribute to the hepatic regulation of iron inhibitor hepcidin (Hamp) [6].

Tfr2-KI and Tfr2 LCKO-KI animal models present germinal and conditional silencing of the Tfr2 gene isoforms Tfr2 α and Tfr2 β [7]. Both the Tfr2 targeted mice, in fact, have a germinal silencing of Tfr2 β isoform, but Tfr2 LCKO-KI animals have an additional hepatic selective silencing of the Tfr2 α isoform as well. While Tfr2-KI mice have normal liver iron amount and normal serum iron parameters (serum ferritin and transferrin saturation), LCKO-KI mice have a severe hepatic iron overload and increased serum iron parameters [7].

Since hearts from *Hfe KO* mice, another animal model of systemic iron overload, had an higher damage after I/R procedure [31], we decided to investigate if cardiac iron metabolism perturbation due to Tfr2 β targeting had some effect on I/R damage, regardless whether hearts have been or not exposed to a systemic iron overload.

We have found, for the first time, that: 1) Tfr2 β protein is significantly increased after I/R in WT mice and that the lack of Tfr2 β expression increased cardiac I/R tolerance, irrespective of systemic iron overload which triggers signs of pre-ischemic apoptosis; 2) while Tfr2 β silencing does not modify HIC levels, it modifies the expression of main iron proteins; 3) Tfr2 β silencing modifies levels of antioxidants, and iron-oxygen dependent enzymes (HO1 and HIF-2a), and the activity of survival (RISK/SAFE) kinases (Table 1).

Although the levels of systemic iron amount are different in the two strains, both Tfr2 β null mice result to have a different cardioprotected-like molecular phenotype.

Indeed, the systemic iron overload affects the level of pre-ischemic apoptosis and, in fact, signs of apoptosis level (BCL S/L) were higher in Tfr2 LCKO-KI hearts than Tfr2-KI. The increased levels of pro-apoptotic factors present in Tfr2 LCKO-KI hearts might be explained by a cell damage due to slight/transient cellular iron overload repeated over time (see below). Nevertheless, after I/R protocol, the infarct size is significantly reduced in both Tfr2 β null mice and these results are associated to different modifications of iron proteins, enzymatic setting and activation of HO-1, HIF-2a and RISK

and/or SAFE pathways in the two transgenic models in response to I/R (see below). Yet, there are no signs of increased apoptosis after I/R in the two models. This can be explainable with the time required to develop apoptosis and with the fact that post-ischemic cells undergoing apoptosis are relatively few compared to necrotic cells [32].

Although we performed repeated measure of HIC, we could not quantitatively demonstrate an increase in iron amount within the myocardium, but several *iron proteins* are modified in Tfr2 LCKO-KI hearts. This is in line with a modified cellular iron trafficking that may cause transient iron stress, repeated over time. In fact, Tfr2 LCKO-KI hearts have an increased iron importer DMT1, an increased cardiac Hamp transcription and a decreased cardiac iron exporter Fpn1 transcription (Table 1), which all together may induce a transient iron overload.

Previous data in splenic macrophages demonstrated the transcriptional correlation between Tfr2 β and the iron exporter Fpn1, since in Tfr2 β null mice a significant decrease in Fpn1 transcription was observed [7]. The Tfr2 β -dependent Fpn1 regulation is also confirmed in heart. In fact, Fpn1 transcription is lower in both Tfr2 β null mice. Therefore, Tfr2 β isoform inactivation could decrease iron release from cells up-regulating somehow the protective pathway including main iron proteins Ferritins (FtH and FtL). These proteins resulted specifically increased even in untreated Tfr2 β null mice, as also found in preconditioned hearts [33]. Actually, a significant increased FtL amount is present in LCKO-KI hearts, probably as a response to the increased free cellular iron through the Iron Responsive Elements /Iron Regulatory Proteins (IRE/IRP) system [21]. This particular result is in agreement with the reported increase of brain FtL transcripts in iron-supplemented mice, which displayed no changes in gross brain iron content [34]. Therefore, our conclusion is that Tfr2 LCKO-KI hearts display an higher tolerance to I/R stress, similarly to that triggered by iron and mediated by ferritin [35].

Different is the situation in Tfr2-KI hearts, which could be protected by FtH higher levels. In fact, while FtL is increased in LCKO-KI I/R, FtH is significantly increased in Tfr2-KI Sham; further supporting different pathway activation in the two Tfr2 targeted models. Several recent studies

demonstrated that the two Ferritin subunits are differently regulated as a response to different stimuli [36]. While FtL subunit appears to be more regulated by iron amount through the IRE/IRP system [21], FtH is more responsive to the presence of oxidant agents either in *in vitro* [37,38] and in *ex vivo* [39] conditions.

Overall, our results suggest that proteins controlling iron trafficking are mainly altered by high systemic iron amount, rather than by lack of Tfr2 beta isoform itself (aside FtH which increased in Tfr2-KI, other iron proteins are significantly increased in LCKO-KI only). Although these variations of proteins suggest that iron trafficking in the cardiac cells is different in the two models, both models are cardioprotected. Therefore we can argue that the antioxidant and pro-survival armamentarium of cardiomyocytes is more ready to limit I/R injury (see below) and/or the metal is in some way less available for ROS production during I/R. Nevertheless, further experiments which also consider iron trafficking in specific cell types (*e.g.*, macrophages, endothelial cells and cardiomyocytes) would be necessary to deepening the role of iron proteins in the mechanisms of cardioprotection.

Since it is well known that the generation of ROS is influenced by iron and that ROS production may play a role either in I/R injury [40,41] or preconditioning protection [35], *via* modulation of *antioxidant enzymes* [35,40-42], SOD1 and Catalase have been evaluated. We observe a different amount of the two enzymes in Sham hearts respect to WT. While SOD1 is not significantly modified in Tfr2 β null hearts (data not shown), Catalase is increased only in Tfr2 LCKO-KI hearts. Again, this result supports, the hypothesis of repeated sublethal iron overload and stress strong enough to upregulate Catalase expression in Tfr2 LCKO-KI hearts only.

The recent discovery that HIF2a contains an iron responsive element (IRE) has underlined the importance of HIF2a as a major player in iron metabolism and protective adaptation to iron stress [20]. Intriguingly, Sham hearts of both models result to have an higher level of two protective factors, namely HO-1 and HIF-2a. This resembles HIF-2a upregulation induced by cardiac ischemic preconditioning, which can be mimicked by the addition of ROS [43] and is in line with the fact that these proteins are influenced by iron dependent redox conditions [20]. It is likely that both transgenic

models have endured an iron/redox stress that led them to react with an increase in cardiac HO-1 and HIF-2 α , thus orchestrating an adaptive response to oxygen deprivation making the heart protected against subsequent damaging stimuli, like I/R.

Since both the Tfr2 β null mice hearts result to be cardioprotected, we also studied the RISK/SAFE pathways. We observed that the two models present some differences in the activation of RISK- and SAFE-pathway. In particular, we observe that starting from similar levels of phosphorylation of *RISK kinases* (AKT, ERK 1/2 and PKC ϵ), the I/R procedure induces an up-regulation of the phosphorylation of these kinases in Tfr2-KI hearts only. The *SAFE pathway* element, Stat3, seems upregulated in Tfr2-KI Sham hearts with respect to WT group, but the I/R procedure induces Stat3 phosphorylation in Tfr2 LCKO-KI only. Intriguingly, this model responds to I/R with an increased phosphorylation of GSK3 β , a putative down-stream kinase of protective pathways, whose role remains still controversial [44,45]. Therefore, it seems that one model (Tfr2-KI) relies mainly on the activation of RISK and the other (LCKO-KI) on the activation of SAFE. Actually these two pathways may be alternative or may cross-talk [11, 14, 15]. We have previously shown that redox conditions may influence the activation of one or the other of these two protective pathways [16]. Since, here we observe differences in terms of iron metabolism in the two models, we can argue that this difference may influence the I/R response to direct the heart towards one or the other of these two pathways. Further studies are necessary to ascertain this point.

4.1. Methodological considerations

This study is realized using the isolated heart model (Langendorff) that is highly adaptable and independent by external cardiac influence [46]. In fact, this model allows to study the intrinsic property of the heart and the capacity of the myocardium to afford a stressful stimulus in a strictly controlled environment, avoiding extra-cardiac influences and the possible effect of temperature and collateral flow variations. The use of the Langendorff model allow us to keep under strict control several factors (*e.g.* heart temperature and perfusion) and to eliminate the confounding effect of systemic factors, including those due to *iron overload* in the remainder of the animal during

experimental maneuvers. Since the relevant comparison is between each transgenic model with its correspondent Sham group, for statistical analysis we used a Student *t* test (unpaired, 2 tailed), and a multi-group comparison by ANOVA was considered not informative.

4.2. Conclusions

Clearly, the hearts of the two Tfr2 β null mice have a different cardiac status and enzymatic setting. It is likely that Tfr2 β silencing causes a modification of iron handling in the cells, which may induce a selective activation of different proteins involved in cell survival. In fact, the myocardium of these two strains results to have different levels of basal pro-apoptotic factors, which seems correlated with systemic iron overload, and to be enriched of specific *iron protein tool kit*, *antioxidant enzymes* and *kinases* involved in cardioprotective pathways ready to be activated after stressful stimuli. In fact Tfr2 β null mice's hearts develop a greater resistance against acute I/R challenge, irrespective of systemic iron content. Further studies are necessary to ascertain the main mechanism of protection and in particular to ascertain whether tissue damage is due to pre-existing adaptations or due to dynamic alteration in iron efflux during the stressful stimuli.

Acknowledgements

This paper was supported in part by Progetti di Ateneo/CSP 2012 (TO_Call3_2012_0101) and AIRC (IG2011 cod 12141) to GS, Progetti di Ateneo/CSP 2012 (TO_Call1_2012_0088) to MDG and Progetti di Ateneo ex60% MeccaSaric to PP and CP.

We are indebted to our colleague Sonia Levi for providing us anti Ferritins antibodies and for fruitful discussions. We also thank Prof Donatella Gattullo for the invaluable support and Saveria Femminò for technical assistance.

The authors have no conflicts of interest to declare.

References

1. Ganz, T. (2013) Systemic iron homeostasis. *Physiol. Rev.* **93**, 1721-1741.
2. Pagliaro, P., Moro, F., Tullio, F., Perrelli, M.G., and Penna, C. (2011) Cardioprotective pathways during reperfusion: focus on redox signaling and other modalities of cell signaling. *Antioxid. Redox Signal.* **14**, 833-850.
3. Xu, J., Marzetti, E., Seo, A.Y., Kim, J.S., Prolla, T.A., et al. (2010) The emerging role of iron dyshomeostasis in the mitochondrial decay of aging. *Mech. Ageing Dev.* **131**, 487-493.
4. Murphy, C.J., and Oudit, G.Y. (2010) Iron-overload cardiomyopathy: pathophysiology, diagnosis, and treatment. *J. Card. Fail.* **16**, 888-900.
5. Kawabata, H., Yang, R., HIRAMA, T., Vuong, P.T., Kawano, S., et al. (1999) Molecular cloning of Transferrin Receptor 2. A new member of the transferrin receptor-like family. *J. Biol. Chem.* **274**, 20826-2032.
6. Hentze, M.W., Muckenthaler, M.U., Galy, B., and Camaschella, C. (2010). Two to tango: regulation of Mammalian iron metabolism. *Cell* **142**, 24-38.
7. Roetto, A., Di Cunto, F., Pellegrino, R.M., Hirsch, E., Azzolino, O., et al. (2010) Comparison of 3 Tfr2-deficient murine models suggests distinct functions for Tfr2-alpha and Tfr2-beta isoforms in different tissues. *Blood* **115**, 3382-3389.
8. Merle, U., Fein, E., Gehrke, S.G., Stremmel, W., and Kulaksiz, H. (2007) The iron regulatory peptide hepcidin is expressed in the heart and regulated by hypoxia and inflammation. *Endocrinology* **148**, 2663-2668.
9. Qian, Z.M., Chang, Y.Z., Leung, G., Du, J.R., Zhu, L., et al. (2007) Expression of ferroportin1, hephaestin and ceruloplasmin in rat heart. *Biochim. Biophys. Acta* **1772**, 527-532.
10. Boengler, K., Hilfiker-Kleiner, D., Heusch, G., and Schulz, R. (2010) Inhibition of permeability transition pore opening by mitochondrial STAT3 and its role in myocardial ischemia/reperfusion. *Basic Res. Cardiol.* **105**, 771-785.
11. Hausenloy, D.J., Lecour, S., and Yellon, D.M. (2011) Reperfusion injury salvage kinase and survivor activating factor enhancement prosurvival signaling pathways in ischemic postconditioning: two sides of the same coin. *Antioxid. Redox Signal.* **14**, 893-907.
12. Penna, C., Brancaccio, M., Tullio, F., Rubinetto, C., Perrelli, M.G., et al. (2014). Overexpression of the muscle-specific protein, melusin, protects from cardiac ischemia/reperfusion injury. *Basic Res. Cardiol.* **109**, 418.
13. Roubille, F., Combes, S., Leal-Sanchez, J., Barrère, C., Cransac, F., et al. (2007) Myocardial expression of a dominant-negative form of Daxx decreases infarct size and attenuates apoptosis in an in vivo mouse model of ischemia/reperfusion injury. *Circulation* **116**, 2709-2717.

14. Heusch G. (2015) Molecular basis of cardioprotection: Signal transduction in ischemic pre-, post-, and remote conditioning. *Circ. Res.* **116**, 674-699.
15. Penna, C., Granata, R., Tocchetti, C.G., Gallo, M.P., Alloatti, G., and Pagliaro, P. (2015) Endogenous Cardioprotective Agents: Role in Pre and Postconditioning. *Curr. Drug. Targets.* **16**, 843-867.
16. Penna, C., Perrelli, M.G., Tullio, F., Angotti, C., Camporeale, A., et al. (2013) Diazoxide postconditioning induces mitochondrial protein S-nitrosylation and a redox-sensitive mitochondrial phosphorylation/translocation of RISK elements: no role for SAFE. *Basic Res. Cardiol.* **108**, 371.
17. Nadtochiy, S.M., Yao, H., McBurney, M.W., Gu, W., Guarente, L., et al. (2011) SIRT1-mediated acute cardioprotection. *Am. J. Physiol. Heart. Circ. Physiol.* **301**, H1506-H1512.
18. Penna, C., Perrelli, M.G., Tullio, F., Angotti, C., and Pagliaro, P. (2013) Acidic infusion in early reperfusion affects the activity of antioxidant enzymes in postischemic isolated rat heart. *J. Surg. Res.* **183**, 111-118.
19. Penna, C., Angotti, C., and Pagliaro, P. (2014). Protein S-nitrosylation in preconditioning and postconditioning. *Exp Biol Med (Maywood)* **239**, 647-662.
20. Simpson, R.J., and McKie, A.T. (2015) Iron and oxygen sensing: a tale of 2 interacting elements? *Metallomics* **7**, 223-231.
21. Muckenthaler, M.U., Galy, B., and Hentze, M.W. (2008) Systemic iron homeostasis and the iron responsive element/iron-regulatory protein (IRE/IRP) regulatory network. *Annu. Rev. Nutr.* **28**, 197-213.
22. Bondi, A., Valentino, P., Daraio, F., Porporato, P., Gramaglia, E., et al. (2005) Hepatic expression of hemochromatosis genes in two mouse strains after phlebotomy and iron overload. *Haematologica* **90**, 1161-1167.
23. Penna, C., Pasqua, T., Perrelli, M.G., Pagliaro, P., Cerra, M.C., et al. (2012) Postconditioning with glucagon like peptide-2 reduces ischemia/reperfusion injury in isolated rat hearts: role of survival kinases and mitochondrial KATP channels. *Basic Res. Cardiol.* **107**, 272.
24. Livak, K.J., and Schmittgen, T.D. (2001) Analysis of Relative Gene Expression Data Using Real-Time Quantitative PCR and the 2- $\Delta\Delta$ CT Method. *Methods* **25**, 402-408.
25. Quail, E.A., and Yeoh, G.C. (1995) The effect of iron status on glyceraldehyde 3-phosphate dehydrogenase expression in rat liver. *FEBS Lett.* **359**, 126-128.
26. Chao, D.T., and Korsmeyer, S.J. (1998) BCL-2 family: regulators of cell death. *Annu. Rev. Immunol.* **16**, 395-419.

27. Ryter, S.W., and Choi, A.M. (2002) Heme oxygenase-1: molecular mechanisms of gene expression in oxygen-related stress. *Antioxid Redox Signal.* **4**, 625-632.
28. Gozzelino, R., Jeney, V., and Soares, M.P. (2010) Mechanisms of cell protection by heme oxygenase-1. *Annu. Rev. Pharmacol. Toxicol.* **50**, 323-354.
29. Wu, M.L., Ho, Y.C., and Yet, S.F. (2011) A central role of heme oxygenase-1 in cardiovascular protection. *Antioxid. Redox Signal.* **15**, 1835-1846.
30. Roetto, A., and Camaschella, C. (2005) New insights into iron homeostasis through the study of non-HFE hereditary haemochromatosis. *Best Pract. Res. Clin. Haematol.* **18**, 235-250.
31. Turoczi, T., Jun, L., Cordis, G., Morris, J.E., Maulik, N., et al. (2003) Mutation and dietary iron content interact to increase ischemia/reperfusion injury of the heart in mice. *Circ. Res.* **92**, 1240-1246.
32. Ferdinandy, P., Schulz, R., and Baxter, G.F. (2007) Interaction of cardiovascular risk factors with myocardial ischemia/reperfusion injury, preconditioning, and postconditioning. *Pharmacol. Rev.* **59**, 418-458.
33. Bulvik, B.E., Berenshtein, E., Meyron-Holtz, E.G., Konijn, A.M., and Chevion, M. (2012) Cardiac protection by preconditioning is generated via an iron-signal created by proteasomal degradation of iron proteins. *PLoS One* **7**, e48947.
34. Johnstone, D., and Milward, E.A. (2010) Genome-wide microarray analysis of brain gene expression in mice on a short-term high iron diet. *Neurochem. Int.* **56**, 856-863.
35. Chevion, M., Leibowitz, S., Aye, N.N., Novogrodsky, O., Singer, A., et al. (2008) Heart protection by ischemic preconditioning: a novel pathway initiated by iron and mediated by ferritin. *J. Mol. Cell. Cardiol.* **45**, 839-845.
36. Arosio, P., and Levi, S. (2010) Cytosolic and mitochondrial ferritins in the regulation of cellular iron homeostasis and oxidative damage. *Biochem. Biophys. Acta* **1800**, 783-792.
37. Cozzi, A., Corsi, B., Levi, S., Santambrogio, P., Albertini, A., and Arosio, P. (2000) Overexpression of wild type and mutated human ferritin H-chain in HeLa cells: in vivo role of ferritin ferroxidase activity. *J. Biol. Chem.* **275**, 25122-25129.
38. Epsztejn, S., Glickstein, H., Picard, V., Slotki, I.N., Breuer, W., et al. (1999) H-ferritin subunit overexpression in erythroid cells reduces the oxidative stress response and induces multidrug resistance properties. *Blood* **94**, 3593-3603.
39. Darshan, D., Vanoaica, L., Richman, L., Beermann, F., and Kühn, L.C. (2009) Conditional deletion of ferritin H in mice induces loss of iron storage and liver damage. *Hepatology* **50**, 852-860.

40. Bolli, R., Dawn, B., Tang, X.L., Qiu, Y., Ping, P., et al. (1998) The nitric oxide hypothesis of late preconditioning. *Basic Res. Cardiol.* **93**, 325-338.
41. Tullio, F., Angotti, C., Perrelli, M.G., Penna, C., and Pagliaro, P. (2013) Redox balance and cardioprotection. *Basic Res. Cardiol.* **108**, 392.
42. Leonarduzzi, G., Sottero, B., Testa, G., Biasi, F., and Poli, G. (2011) New insights into redox-modulated cell signaling. *Curr. Pharm. Des.* **17**, 3994-4006.
43. Bautista, L., Castro, M.J., López-Barneo, J., and Castellano, A. (2009) Hypoxia inducible factor-2alpha stabilization and maxi-K⁺ channel beta1-subunit gene repression by hypoxia in cardiac myocytes: role in preconditioning. *Circ. Res.* **104**, 1364-1372.
44. Heusch, G., and Schulz, R. (2009) Neglect of the coronary circulation: some critical remarks on problems in the translation of cardioprotection. *Cardiovasc. Res.* **84**, 111-114.
45. Lacerda, L., Somers, S., Opie, L.H., and Lecour, S. (2009) Ischaemic postconditioning protects against reperfusion injury via the SAFE pathway. *Cardiovasc. Res.* **84**, 201-208.
46. Bell, R.M., Mocanu, M.M., and Yellon, D.M. (2011) Retrograde heart perfusion: the Langendorff technique of isolated heart perfusion. *J. Mol. Cell. Cardiol.* **50**, 940-950.

Titles and legends to figures

FIGURE 1 Molecular detection of Tfr2 β in WT mice in Sham and after I/R protocols. Infarct size and molecular detection of BCL-X S/L, HO-1 and HIF-2a in WT and Tfr2 targeted mice in Sham and after I/R protocols.

- a) Western blot (WB) analysis for Tfr2 β was performed on lysate from left ventricles (LV) collected at the end of protocols in Sham and I/R WT animals. An increase of Tfr2 β is observed in WT I/R mice vs WT Sham. T β : transfected Tfr2 β isoform used as positive control.
- b) Infarct size (IS), expressed as percentage of LV, resulted smaller in Transgenic models compared with WT I/R mice. Animals between 5 and 7 (see Methods).
- c) WB analysis for BCL-X S/L is obtained as ratio between S and L subunits production.
- d) and e) WB analysis for HO-1 and HIF-2a were performed on lysates from LV collected at the end of protocols WT and targeted mice (KI and LCKO-KI).

Graph represents the densitometric analysis of protein normalized to Gapdh and reported as relative fold increase. Blots images: vertical lines indicate images taken from different gels. All WB analyses were carried out in triplicate. *p < 0.05, **p < 0.01.

FIGURE 2: Molecular detection of RISK pathway in WT and Tfr2 targeted mice, in Sham and after I/R protocols.

Western blot analysis was performed on lysates from LV collected at the end of protocols of WT and targeted mice (KI and LCKO-KI). RISK pathway proteins investigated: a) ERK1/2; b) AKT and c) PKC ϵ . Graphs represent the densitometric analysis of phosphorylated proteins normalized to total proteins and reported as relative fold increase Blots images: vertical lines indicate images taken from different gels. All analyses were carried out in triplicate. *p < 0.05, **p < 0.01, ***p < 0.001.

FIGURE 3: Molecular detection of SAFE pathway and GSK3 β in WT and Tfr2 targeted mice in Sham and after I/R protocols.

Western blot analysis was performed on lysates from LV collected at the end of protocols of WT and targeted mice (KI and LCKO-KI). SAFE pathway proteins investigated are a) Stat3 and b) GSK3 β . Graphs represent the densitometric analysis of phosphorylated proteins normalized to total proteins and reported as relative fold increase. Blots images: vertical lines indicate images taken from different gels. All analyses were carried out in triplicate. * $p < 0.05$, ** $p < 0.01$.

FIGURE 4: Molecular detection of Catalase in WT and Tfr2 targeted mice in Sham and after I/R protocols.

Western blot analysis was performed on lysates from LV collected at the end of protocols of WT and targeted mice (KI and LCKO-KI). Graphs represent the densitometric analysis of proteins normalized to Gapdh and reported as relative fold increase. Blots images: vertical lines indicate images taken from different gels. All analyses were carried out in triplicate. * $p < 0.05$.

FIGURE 5: Cardiac iron genes expression and molecular detection of DMT1 in WT and Tfr2 targeted mice in Sham and after I/R protocols.

Cardiac relative expression of iron genes a) Hamp and b) Fpn1. Gene expression analysis was performed on LV collected at the end of protocols of WT and targeted mice (KI and LCKO-KI). c) DMT1 Western blot analysis was performed on lysates from LV collected at the end of protocols of WT and targeted mice (KI and LCKO-KI). Graph represents the densitometric analysis of protein normalized to Gapdh and reported as relative fold increase. Blots images: vertical lines indicate images taken from different gels. All analyses were carried out in triplicate. ** $p < 0.01$.

FIGURE 6: Heart iron concentration (HIC) and molecular analysis of FtH and FtL in WT and Tfr2 targeted mice in Sham and after I/R protocols.

a) Heart Iron Concentration (HIC) assessment was performed using 20 mg of dried LV collected at the end of protocols in WT and targeted mice (KI and LCKO-KI; n= 4-5).

Western blot analysis (b and c) was performed on lysates from LV collected at the end of protocols WT and targeted mice (KI and LCKO-KI). Graphs represent the densitometric analysis of proteins normalized to Gapdh and reported as relative fold increase. Blot images: vertical lines indicate images taken from different gels. All analyses were carried out in triplicate. * $p < 0.05$, ** $p < 0.01$.

Figure 1A

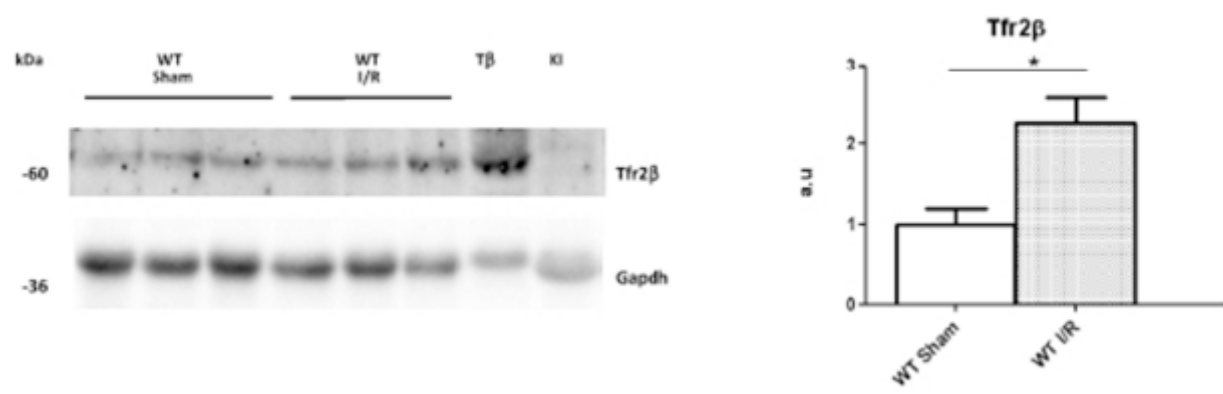


Figure 1B

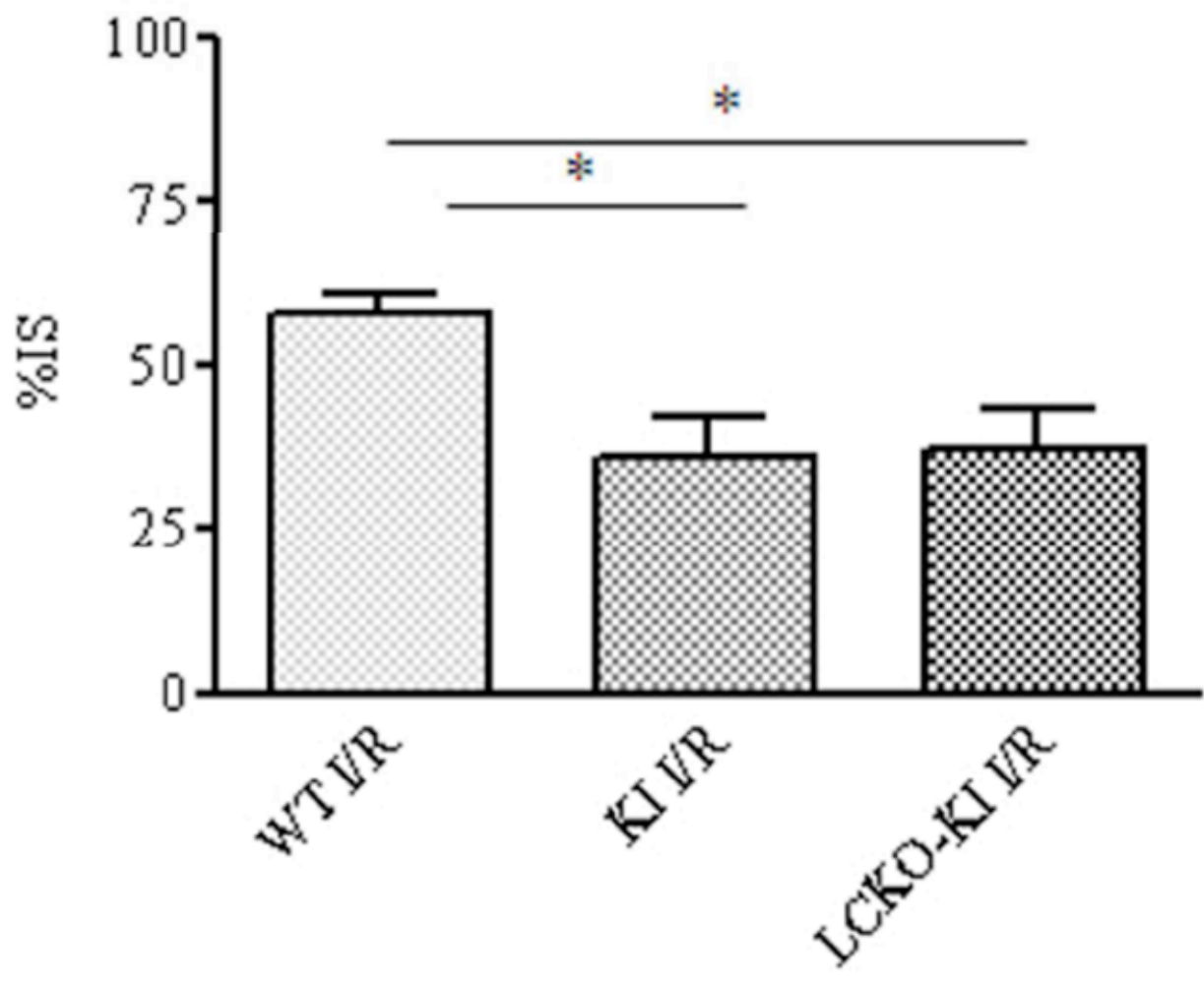


Figure 1C

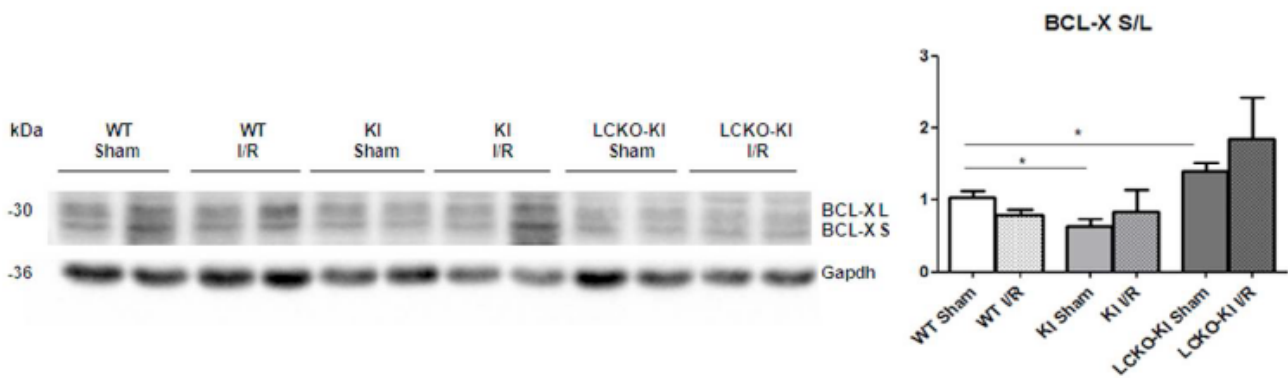


Figure 1D

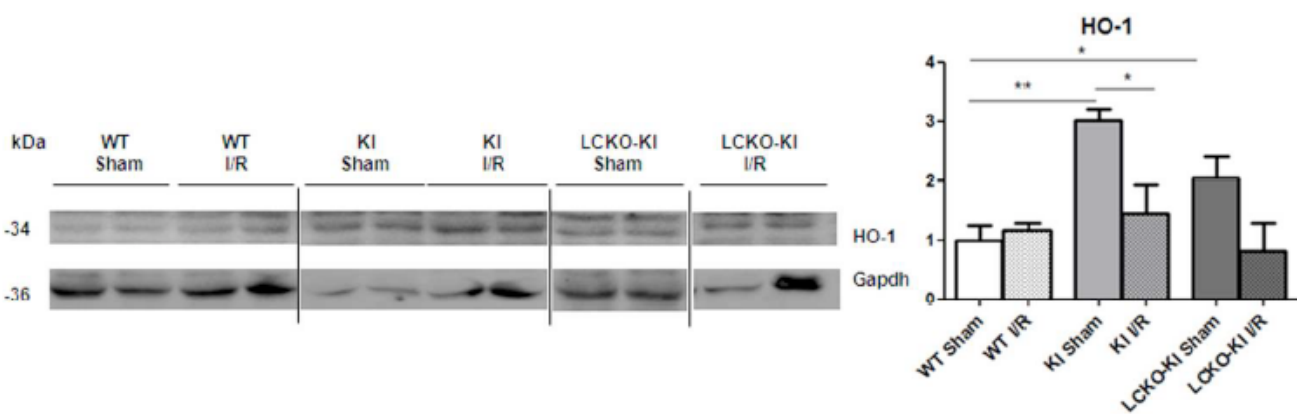


Figure 1E

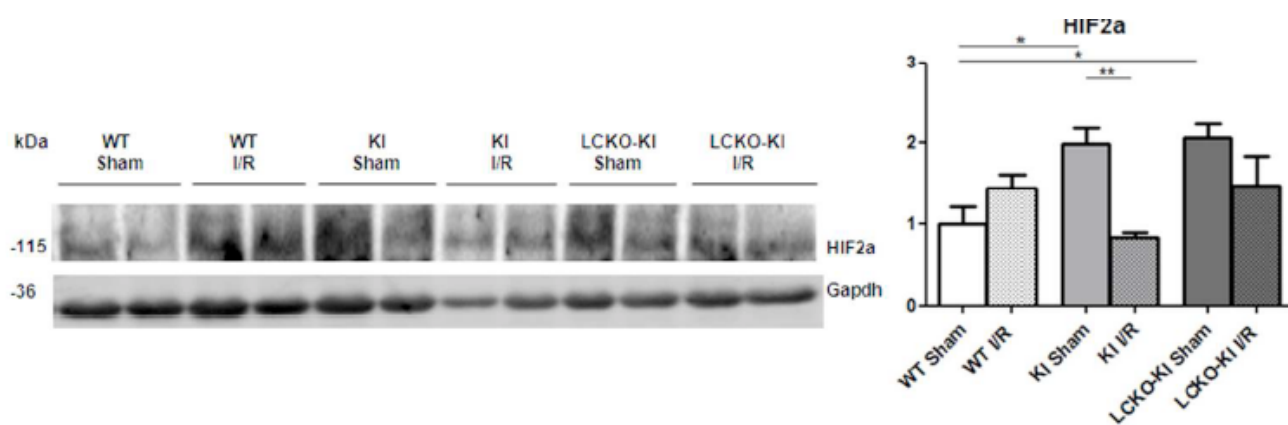
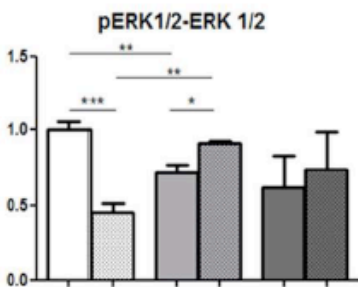
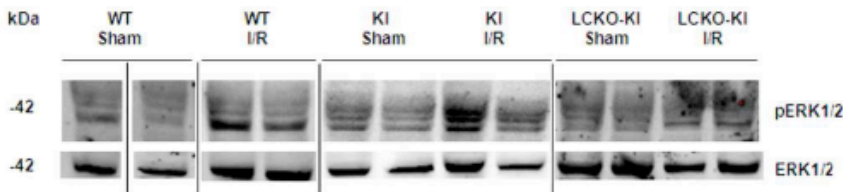


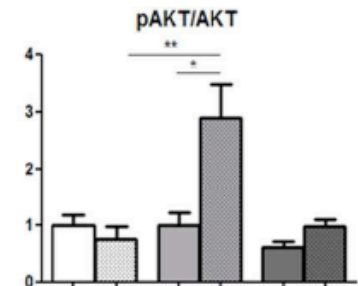
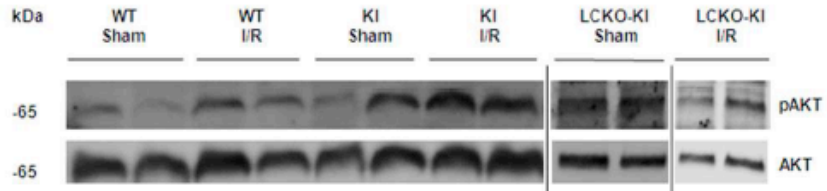
Figure 2

Fig 2

a)



b)



c)

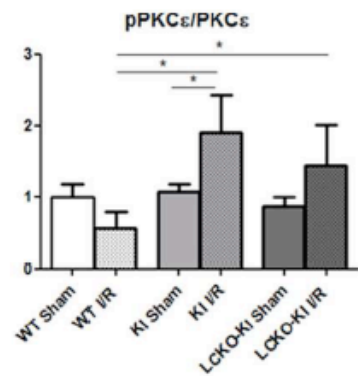
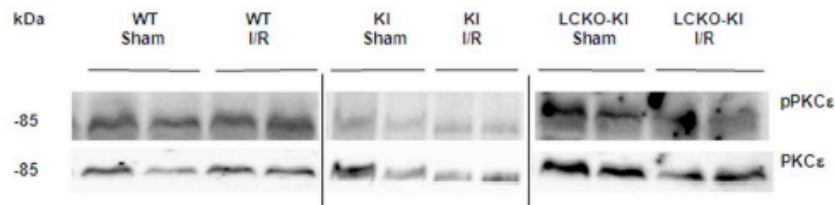


Figure 3

Fig 3

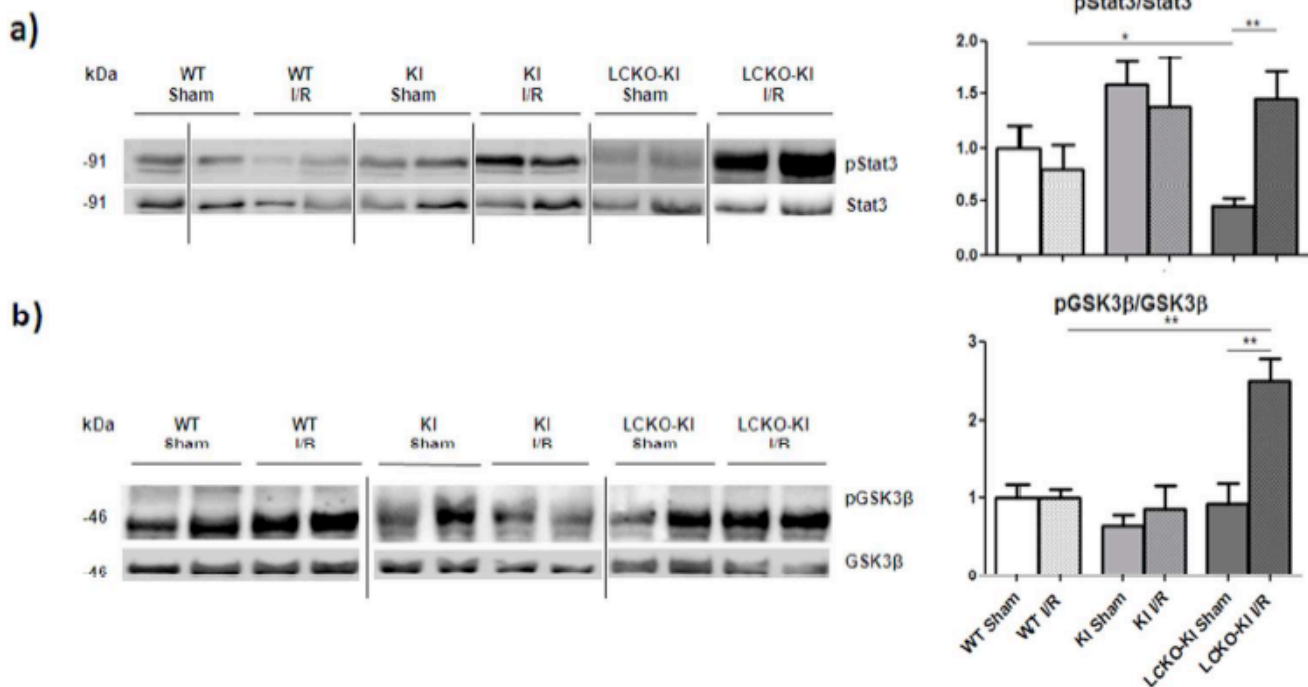


Figure 4

Fig 4

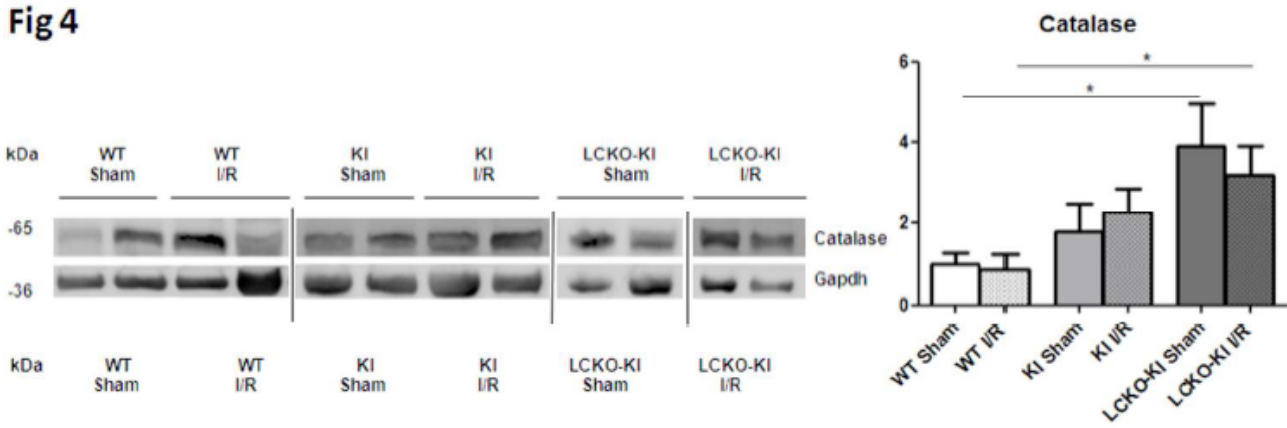
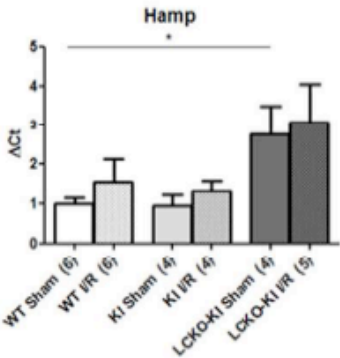


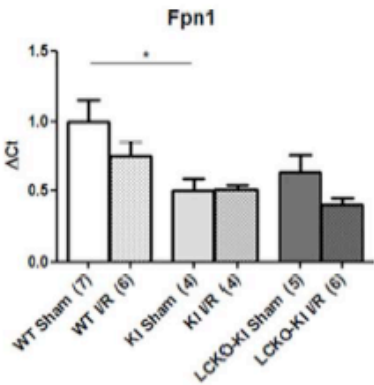
Figure 5

Fig 5

a)



b)



c)

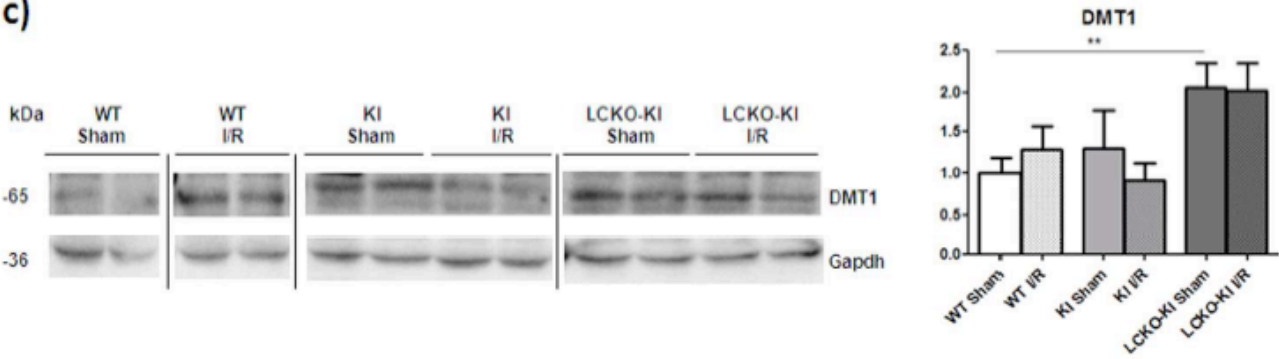
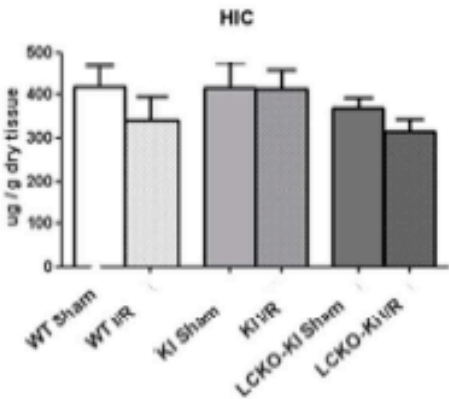
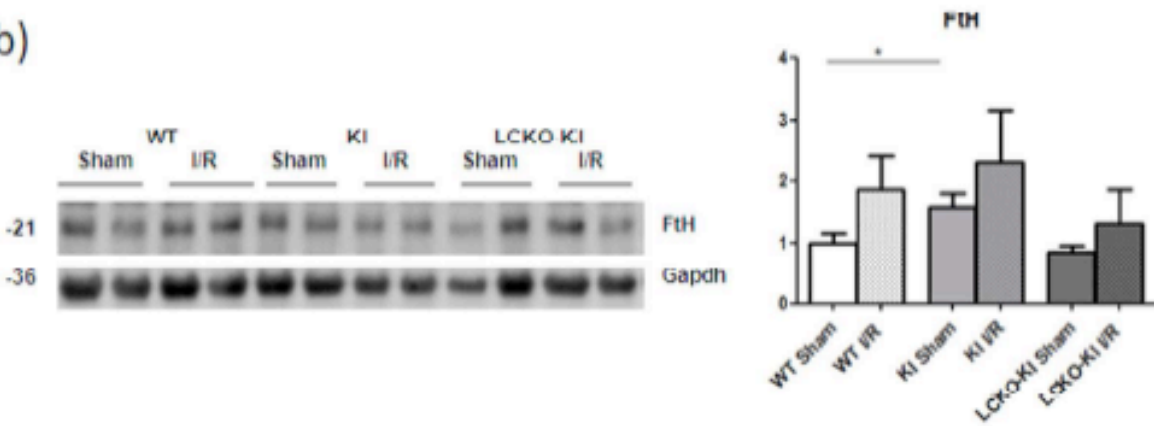


Figure 6

a)



b)



c)

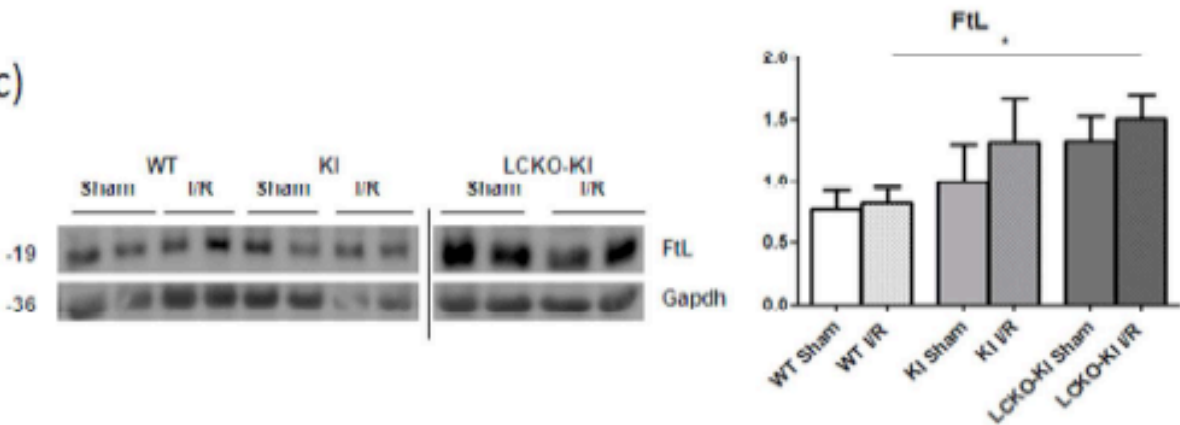


Table 1

Table 1. Variation of analyzed parameters at the end of protocols in WT and targeted mice.

	WILD-TYPE	KI		LCKO-KI	
	I/R	SHAM	I/R	SHAM	I/R
TFR2 β	↑	NA	NA	NA	NA
Infarct size	NA	NA	↓ (WT I/R)	NA	↓ (WT I/R)
BCL S/L	ND	↓	ND	↑	ND
HO-1	ND	↑↑	ND ↓ (KI Sham)	↑	ND
HIF-2	ND	↑	ND ↓↓ (KI Sham)	↑	ND

RISK and SAFE					
pERK1/2/ERK1/2	↓↓↓	↓↓	↑↑ (WT I/R) ↑ (KI Sham)	ND	ND
pAKT/AKT	ND	ND	↑↑ (WT I/R) ↑ (KI Sham)	ND	ND
pPKC ϵ /PKC ϵ	ND	ND	↑ (WT I/R) ↑ (KI Sham)	ND	↑ (WT I/R) ND(LCKO-KI Sham)
pSTAT3/STAT3	ND	ND	ND	↓	ND ↑↑ (LCKO-KI Sham)
pGSK3 β /GSK3 β	ND	ND	ND	ND	↑↑ (WT I/R) ↑↑ (LCKO-KI Sham)

IRON and Proteins					
Hamp (RNA)	ND	ND	ND	↑	ND
Fpn1 (RNA)	ND	↓	ND	ND	ND
DMT1	ND	ND	ND	↑↑	ND
HIC	ND	ND	ND	ND	ND
FtH	ND	↑	ND	ND	ND
FtL	ND	ND	ND	ND	↑ (WT I/R) ND(LCKO-KI Sham)

ANTIOXIDANT ENZYMES					
Catalase	ND	ND	ND	↑	↑ (WT I/R) ND(LCKO-KI Sham)
SOD1	ND	ND	ND	ND	ND

The table shows a summary of the all analyzed parameters at the end of protocols in WT and targeted mice (KI and LCKO-KI). Arrows show variation (↑, ↓ $p < 0.05$; ↑↑, ↓↓ $p < 0.01$; ↓↓↓ $p < 0.001$) with respect to the Sham WT or respect to the group reported in brackets. ND= no difference with respect to Sham WT or respect to the group reported in brackets. NA= not applicable. For acronyms see the text.